Thermal diffusivity measurements of porous CFRP specimens with different number of plies using pulsed thermography in transmission and reflection mode

by G. Mayr*, B. Plank*, J. Gruber*, J. Sekelja** and G. Hendorfer*

* University of Applied Sciences, Stelzhamerstraße 23, A-4600 Wels, Austria, guenther.mayr@fh-wels.at
** FACC AG, Fischerstraße 9, A-4910 Ried im Innkreis, Austria, j.sekelja@facc.com

Abstract

Porosity in carbon fibre reinforced polymers (CFRP) degrades the engineering performance, especially the interlaminar shear strength. In this work the porosity of CFRP was successfully determined by means of pulsed thermography. Additionally cone beam Xray computed tomography (3D-XCT) measurements were carried out. The observation time and the resulting thermal diffusivity were determined for 116 CFRP test specimens with different porosity levels and different numbers of plies. The samples were fabricated using 5 ply, 10 ply and 20 ply laminates, and the specimen thicknesses varied from 1.02 mm to 5.2 mm. The comparison of CFRP specimens with different numbers of plies shows similar results in the dependency of thermal diffusivity on porosity. The results show a very good correlation between transmission and reflection measurement methods. The good correlation between the effective medium theory and the experimental results allows a quantitative evaluation of porosity with pulsed thermography to be made, which yields results comparable to the quality of ultrasonic testing.

1. Introduction

Porosity in carbon fibre reinforced polymers (CFRP) degrades the engineering performance, especially the interlaminar shear strength. The shear strength depends primarily on the mechanical properties of the epoxy matrix, which are weakened by the presence of porosity [1]. In the majority of cases the aviation industry needs to ensure a porosity level lower than 2.5 % for the structural parts. The state-of-the-art method for non-destructive evaluation of porosity in the aviation industry is ultrasonic testing [2].

In contrast to ultrasonic testing, pulsed thermography allows for the rapid non-intrusive inspection of complex-shaped structures and is therefore quite promising with respect to cost reduction. A prior study from Connolly [3] has shown the great potential of active thermography in transmission mode for the detection of porosity in CFRP. He demonstrated that particularly thermal diffusivity imaging reflects inhomogeneous material parameters which correlate roughly linearly to increased porosity. A qualitative study on aircraft components was given by Grinzato et al. [4], who demonstrated a strong agreement between ultrasonic C-Scan, thermal diffusivity and effusivity images. Zalameda and Winfree [5] characterized simulated porosity (hollow carbon spheres) in graphite composites using a phase lag technique to calculate the thermal diffusivity. They demonstrated that a simple electrical analog model allows an estimation of the effective thermal diffusivity changes in graphite composites. A more advanced model which takes the microstructure of the pores into account was introduced as ‘‘Dethermalization Theory’’ by Ringermacher [6,7]. According to this model the microstructural information can be very useful when calculating the thermal conductivity and consequently the thermal diffusivity, as indicated by previous experimental studies [8] and numerical simulations [9].

This work concentrates on 20 ply, 10 ply and 5 ply laminates with porosity levels from 0 % to 18.32 %. To characterize the porosity quantitative thermal diffusivity measurements in transmission and reflection mode were carried out. The relationship between the level of porosity and the change in the thermal diffusivity is analyzed using an effective-medium approximation from Maxwell-Garnett [10] and the weighted average of the volumetric heat capacity. Based on these physical models and microstructure information derived from cone beam Xray computed tomography (3D-XCT) measurements the porosity can be predicted from the measured thermal diffusivity. This approach is verified on a set of different porous CFRP specimens.

2. Heat conduction in porous media

Heterogeneous materials are composed of domains of different materials (phases). In a simplified case of porous CFRP there is a randomly distributed heterogeneous material with two phases: (i) the carbon-epoxy matrix and (ii) the gas filled pores. The term porosity is defined as the volume of pores V_p over the total volume of the material and voids V by the following equation $\Phi = V_p / V$. For the analysis of the macroscopic time-dependent heat flow through a porous material, the effective (or local-volume averaged) properties such as the effective thermal conductivity k_{eff} and effective volumetric heat capacity $(\rho\, c)_{eff}$ are used [10]. The effective thermal conductivity depends on the microstructure of the heterogeneous material as well as on the thermal conductivity of the carbon-epoxy matrix and the gas-filled pores. For the prediction of the effective thermal conductivity of porous CFRP the Maxwell-Garnett Approximation [11] is used

$$k_{\mathrm{eff}} = k_{\mathrm{m}} + \Phi \cdot \left(k_{\mathrm{p}} - k_{\mathrm{m}}\right) \cdot \frac{k_{\mathrm{m}}}{k_{\mathrm{m}} + \eta \cdot \left(k_{\mathrm{p}} - k_{\mathrm{m}}\right) + \Phi \cdot \eta \cdot \left(k_{\mathrm{m}} - k_{\mathrm{p}}\right)} \tag{1}$$

where the subscripts m and p denote respectively the matrix (carbon fibre and epoxy resin) and the pores. The "dethermalization factor" η of an oblate ellipsoid takes the influence of the microstructure into account and depends on the pores aspect ratio m [12]:

$$\eta = \frac{m^2}{m^2 - 1} - \frac{m^2}{\left(m^2 - 1\right)^{3/2}} \arcsin\left(\frac{\left(m^2 - 1\right)^{1/2}}{m}\right) \tag{2}$$

where m is defined as the ratio of the long axes lengths to the short axis length of an oblate ellipsoid ($m = a / b$). The effective volumetric heat capacity is obtained by simple volume averaging:

$$\left(\rho \cdot c\right)_{\mathrm{eff}} = \left(\rho \cdot c\right)_{\mathrm{p}} \cdot \Phi + \left(\rho \cdot c\right)_{\mathrm{m}} \cdot \left(1 - \Phi\right). \tag{3}$$

If the heterogeneous material can be considered homogeneous on transient conditions which means that the thermal wavelength is much longer the microscopic pore scale the thermal diffusivity α can be used as a characteristic constant for the porous material [13]:

$$\alpha_{\mathrm{eff}} = \frac{k_{\mathrm{eff}}}{\left(\rho \cdot c\right)_{\mathrm{eff}}}. \tag{4}$$

Figure 1 (left) shows the dependence of the effective thermal conductivity and volumetric heat capacity on the aspect ratio of the pores and the porosity level. This graph reveals that the effective thermal conductivity and volumetric heat capacity decrease with porosity. An increasing aspect ratio leads to a significant decrease of the thermal conductivity. The effective thermal diffusivity derived from Eq. 4 is plotted versus porosity for three different aspect ratios in figure 1 (right). The calculated values show a strong dependence on the pore shape therefore the microstructure has to be accurately known to allow the prediction of the effective thermal properties of porous CFRP.

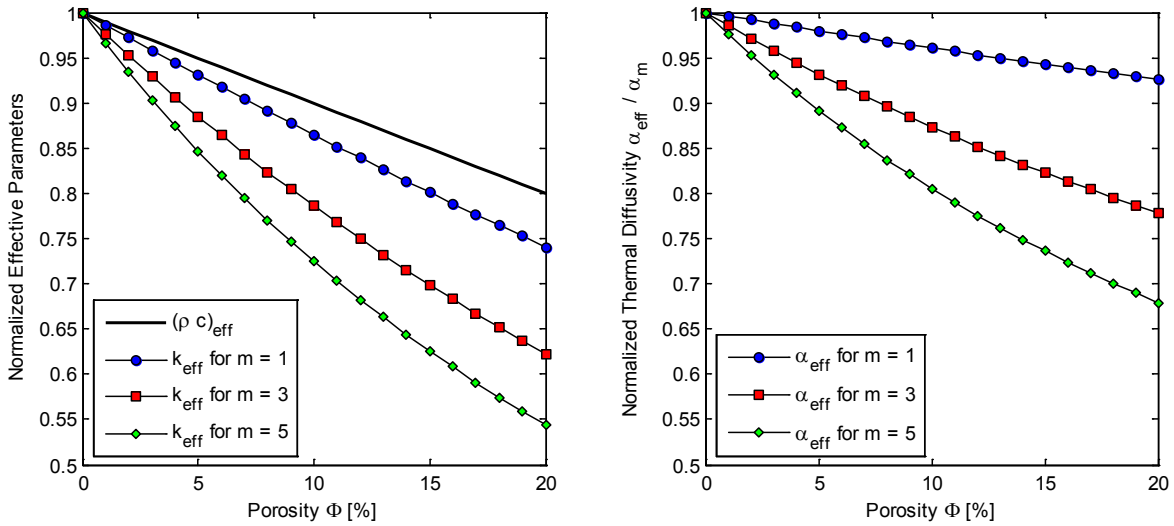

Fig. 1. *A plot of the normalized effective heat conductivity and effective volumetric heat capacity obtained using the Eq. 1 und Eq. 3 for different pore aspect ratios as a function of porosity (left) and the calculated effective thermal diffusivity (Eq. 4) versus porosity (right).*

3. Experiments

3.1. Test specimens

For this study, a prepreg fabric which is widely used in the aerospace industry was chosen. The material is a carbon fibre reinforced polymer (CFRP) which is known as: CYCOM 970 / PWC T300 3 k. The initial fibre volume fraction is 50 % and the weight fraction of resin in the prepreg is 40 %. The densities of prepreg, fibre and uncured resin are also known. The 116 porous samples were fabricated by using 20 ply, 10 ply and 5 ply plain weave style laminate with a single nominal ply thickness of 0.2159 mm. The specimen thicknesses varied due to the porosity level (table 1). To create different amounts and types of pores different cure cycles were selected. For the curing cycle different pressures and temperatures were used to fabricate specimens with various porosities between 0 % and 18.32 %. The sets of samples with a size of 40 mm x 20 mm (P20, P10 and P05) are joined together with hot glue to form three mosaic-like test panels. These test panels were used for the pulsed thermography experiments.

Table 1. *Descriptions of tested porous CFRP specimens.*

Label	*Number of plies*	*Range of thickness* [mm]	*Range of porosity* [%]	*Number of samples*	*Measuring with 3D-XCT*
P20	20	4.25 … 5.30	0 … 18.32	16	16
P10	10	2.12 … 2.58	0 … 16.04	50	12
P05	5	1.02 … 1.14	0 … 5.67	50	12

3.2. Pulsed thermography in transmission and reflection mode

3.2.1. Experimental setup

The pulsed thermography measurement system is shown schematically in figure 2. Flash lamps are used to deposit a controlled heat pulse to one surface of the sample and an infrared camera is used to monitor the surface radiation on the front (reflection mode) and on the back (transmission mode) side of the specimen. The infrared camera uses an indium antimonide FPA detector (320 x 256 pixels) which is sensitive to radiation in the 3.0 – 5.0 µm spectral range. The camera records the data with a frame rate at 50 frames per second and has a NEDT of <20 mK. The flash lamps provide an output power of 6 kJ with a flash duration of approximately 2 ms. By using PMMA Filters, the disturbing infrared heat radiating from the flash lamps head after heating is blocked. A standard PC controls the IR camera, acquires and processes the image data.

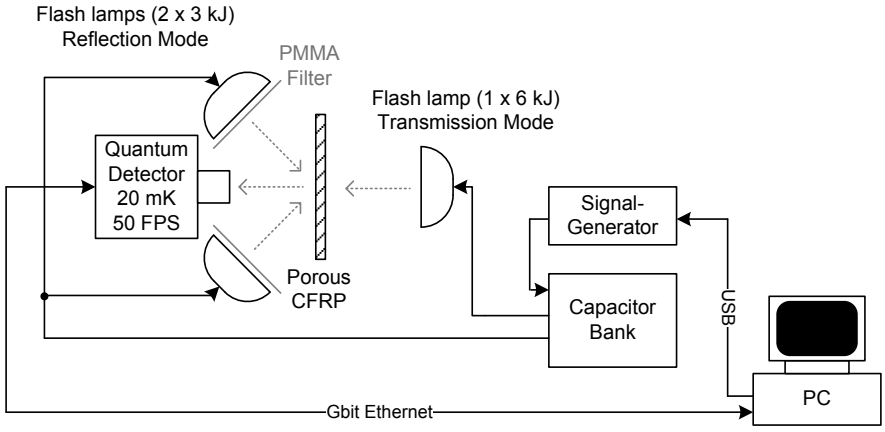

Fig. 2. *Schematic illustration of a pulsed thermography apparatus for non-destructive testing of porous CFRP in reflection and transmission mode.*

3.2.2. Thermal diffusivity measurement approaches

The thermal diffusivity can be obtained by pulsed thermography measurements in transmission and reflection mode. In transmission mode a time-domain procedure is applied which is closely related to the standardized Parker's method [15]. The method used here [16,17] is based on a transformation of the rear face temperature (figure 3-left) in a

semi-logarithmic domain (figure 3-right) of the form of [$ln(T - T_0) + ½\ ln\ (t)$] versus [$1 / t$] to achieve a linearization of the temperature curves. By evaluating the slope K of these linearized plots at time stamps corresponding to approximately 30 % to 80 % of the signal maximum we are able to determine the thermal diffusivity

$$\alpha = -\frac{L^2}{4 \cdot K}, \tag{5}$$

where L is the sample thickness. With this method we separate the effects due to excitation and surface conditions from the effects due to heat diffusion because the deposited energy only affects the y-intercept and not the slope K of the linearized temperature curves.

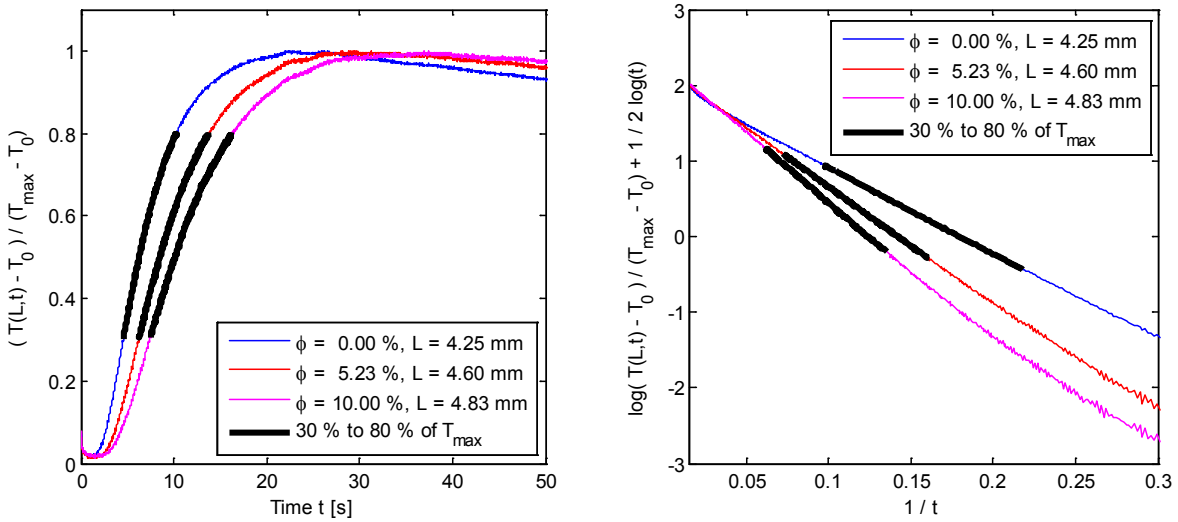

Fig. 3. *Thermal diffusivity measurement in transmission mode: (left) Temperature versus time for three porous CFRP specimens with 20 plies and (right) a linearization of the temperature curves using the logarithmic method. The thick black line shows the interval of temperatures from 30% to 80% of the temperature maximum T_{max}.*

The TSR (Thermographic Signal Reconstruction) method proposed by Shepard [18] is used to predict the thermal diffusivity in reflection mode. In this method the log-log temperature curves (figure 4-left) are approximated by a logarithmic polynomial of order n. The differentiation of the polynomial function allows the computation of the 1st and 2nd derivative without an amplification of the thermal noise. The 1st derivatives inflection point and the 2nd derivatives maxima can be used to estimate the thermal diffusivity. For a precise quantitative evaluation the recommendations of Balageas [19] are applied: 1st logarithmic derivative of the log-log thermogram, logarithmic polynomial of degree 9 and a Fourier number (Fo = α t / L^2) – domain of [0.05 to 1.6]. The Fo - domain is determined from measurement results in transmission mode. In the case of a perfect adiabatic slab the thermal diffusivity is deduced from the inflection point of the 1st derivative. In the case of experimental data and heat losses on the front and back side of the specimen we used the half-rise point t^* of the 1st derivative (figure 4-right) to calculate the thermal diffusivity

$$\alpha = \frac{L^2}{\pi \cdot t^*}. \tag{6}$$

The average disagreement between the measured thermal diffusivity values derived by the two methods is only 0.5 %, the reflection measurement being typically smaller than the transmission measurement. This comparison is validated for homogeneous materials.

3.3. Three dimensional X-ray computed tomography (3D-XCT)

The 3D-XCT experiment is used as a reference standard for the porosity. Additionally the 3D-XCT yields data on the pore dimension in the x, y and z direction. Based on this information the mean aspect ratio for each porosity sample can be obtained. The 3D-XCT device consists of a 180 keV nano-focus tube and a full digital 2300 x 2300 pixel flat panel detector. For the measurements in this study a spatial resolution (voxel size) of 10 µm was used. The evaluation method applied to the 3D-XCT-data to determine the porosity is described in [20], where a global threshold method for segmenting voids in 3D-XCT-data is given. These porosity values derived from 3D-XCT were compared with the results of acid digestion measurements. A linear correlation with a correlation factor of 0.98 can be achieved.

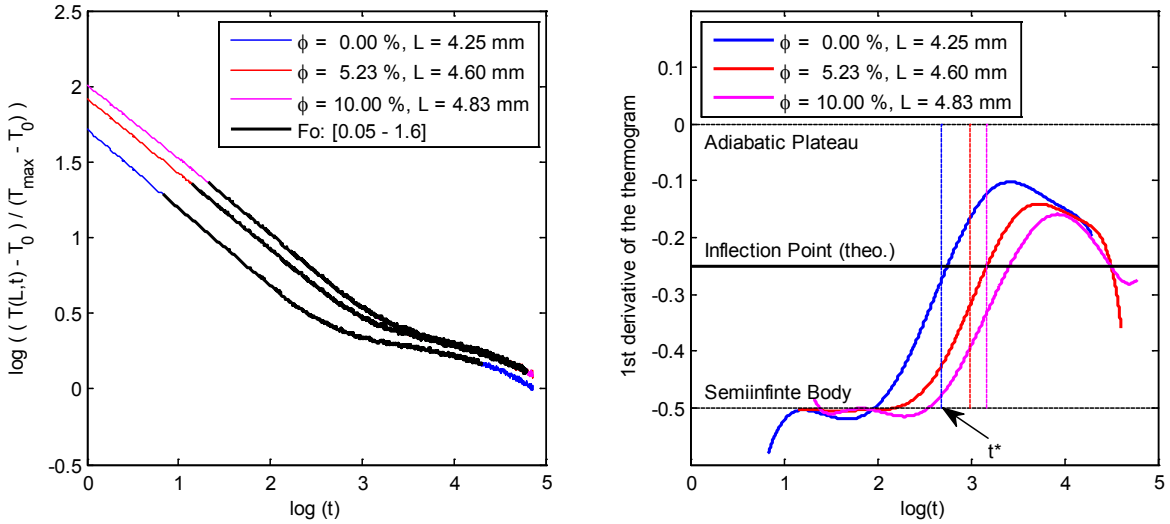

Fig. 4. *Thermal diffusivity measurement in reflection mode: (left) Logarithmic temperature versus logarithmic time for three porous CFRP specimens with 20 plies and (right) the 1st logarithmic derivatives of the log-log temperature curves. The half-rise points t* of the 1st derivatives are indicated by dashed vertical lines.*

4. Experimental Results

4.1. Thermal diffusivity measurement in transmission and reflection mode

Experiments were performed on three different porosity test plates composed of 20 ply, 10 ply and 5 ply laminates. The individual porosity samples (40 mm x 20mm) are joined together by hot glue to form a mosaic-like test panel. To measure the diffusion time ($t_D = L^2 / \alpha$) pulsed thermography experiments in transmission and reflection mode were carried out. As an example the corresponding diffusion time images for the 20 ply test panel are depicted in figure 5. The darkest regions (upper left) represent the lowest values of diffusion time and therefore exhibit very low porosity. Increased porosity levels leads to higher sample thickness and lower thermal diffusivity values, which leads to higher diffusion times (lower right). The diffusion time image obtained in reflection mode looks noisier compared to the one obtained in transmission mode. Furthermore artifacts in the edge regions of the test panel disturb the reflection mode's diffusion time image.

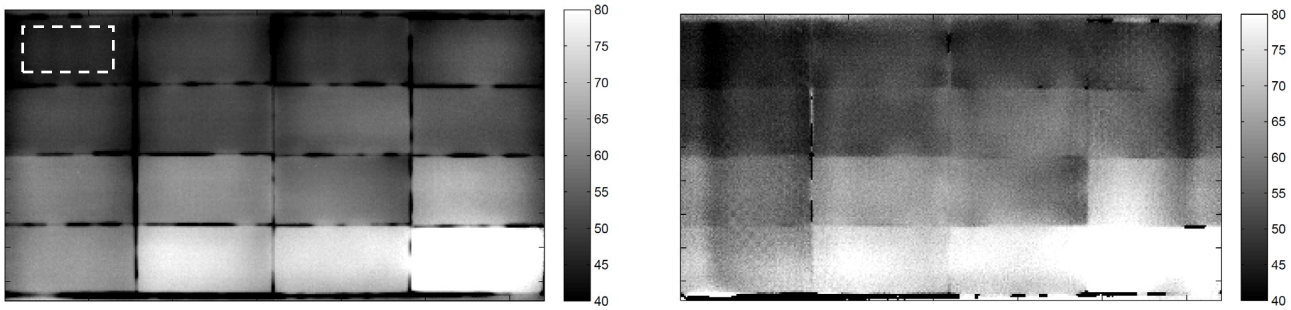

Fig. 5. *Comparison of the diffusion time images ($t_D = L^2 / \alpha$) derived in transmission (left) and reflection (right) mode of the 20 ply test specimens. In the upper left corner the 0 % porosity image is shown. In the lower right corner the 18.32 % porosity sample is located.*

Only the diffusion time values of predefined areas with a size of (40 x 20) pixel in the middle of the porosity samples are evaluated in order to avoid edge effects (see white frame in figure 5-left). The averaged diffusion time values from the predefined areas are used to calculate the effective thermal diffusivity. The effective thermal diffusivity as a function of porosity for 40 test specimens with 20, 10 and 5 plies is shown in figure 6. The results of the samples of different number of plies are relatively consistent, with a decrease in the diffusivity produced by an increase in porosity. The repeatability as shown by the error bars was derived from five independent experiments. It was 10 times better with transmission measurements than with reflection measurements.

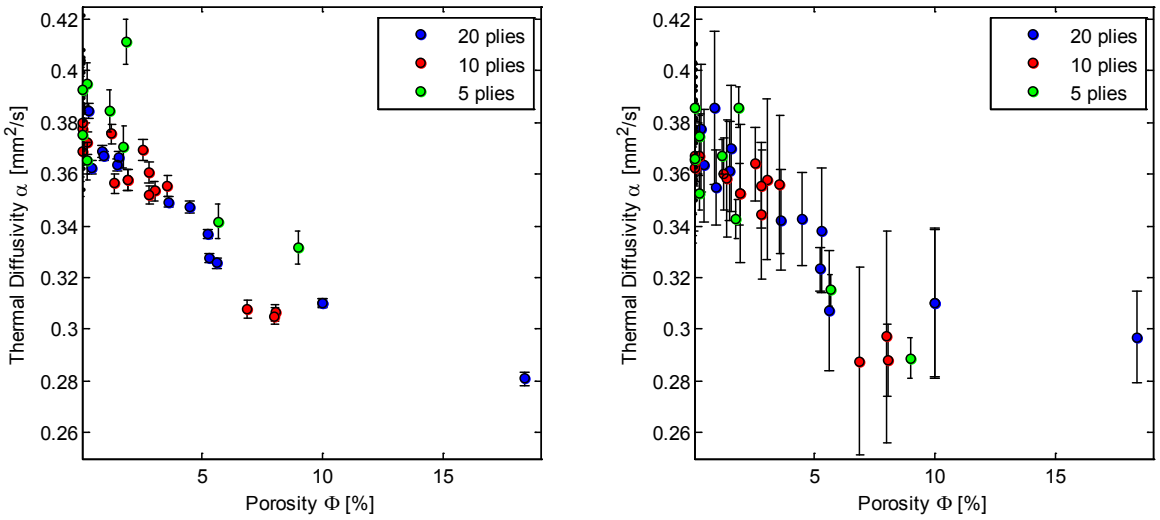

Fig. 6. *A plot of the measured thermal diffusivities in transmission (left) and reflection mode (right) of 20, 10 and 5 plies porosity samples versus porosity obtained by 3D-XCT.*

Figure 7 shows a quantitative comparison between the measured thermal diffusivity values in transmission and reflection mode. A straight line is drawn on the plot to indicate where there is exact agreement between the two experimental setups. The disagreement between the two methods is for the most specimens lower than 5 % (fine dashed lines). The values measured in reflection mode are slightly lower than the transmission mode values, which corresponds with the results of Winfree and Zalameda [21].

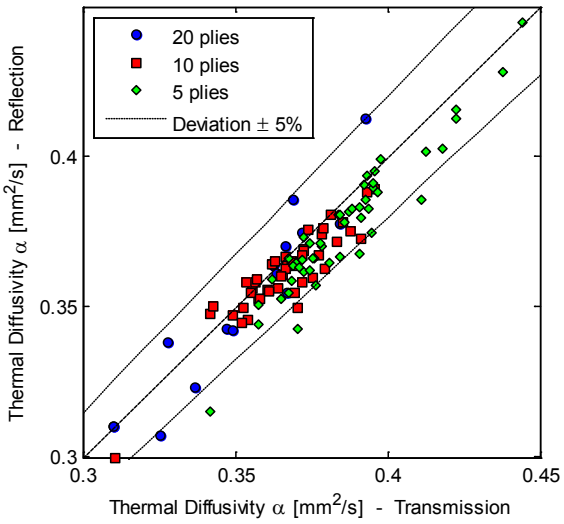

Fig. 7. *Comparison of the measured thermal diffusivity according to pulsed thermography experiments in transmission and reflection mode for CFRP porosity samples with 20, 10 and 5 plies.*

4.2. Microstructure characterization by means of 3D-XCT

To characterize the microstructure 40 test specimens of different porosity levels and quantity of plies were analyzed by means of 3D-XCT. In previous papers [22], the aspect ratio *m* for pores in CFRP was often sets at 1 (sphere). Actually, the pore aspect ratios are not evenly distributed in the sample and their values will change with porosity (figure 8-left). In this study the non-uniform shapes of real pores are idealized to be spheroidal elements with out-of-plane (perpendicular to the fibre bundles) aspect ratios $m_{((x,y)\ /\ z)}$ in the range of approximately 1.5 to 4.5. The

averaged in-plane (parallel to the fibre bundles) aspect ratio $m_{(x\,/\,y)}$ is approximately 1 for all porosity levels. This implies that the pores are on average rotationally symmetrical. The pores can thus be modeled as oblate spheroids. The values of the "dethermalization" factors for the idealized pores given in figure 8 (right) are determined by the aspect ratio $m_{((x,y)\,/\,z)}$ used in Eq. 2. As the porosity increases the pores tend to be flatter and therefore the "dethermalization" factor rises. This phenomenon leads to decreased effective thermal diffusivity values in comparison to spherical pores at the same porosity level.

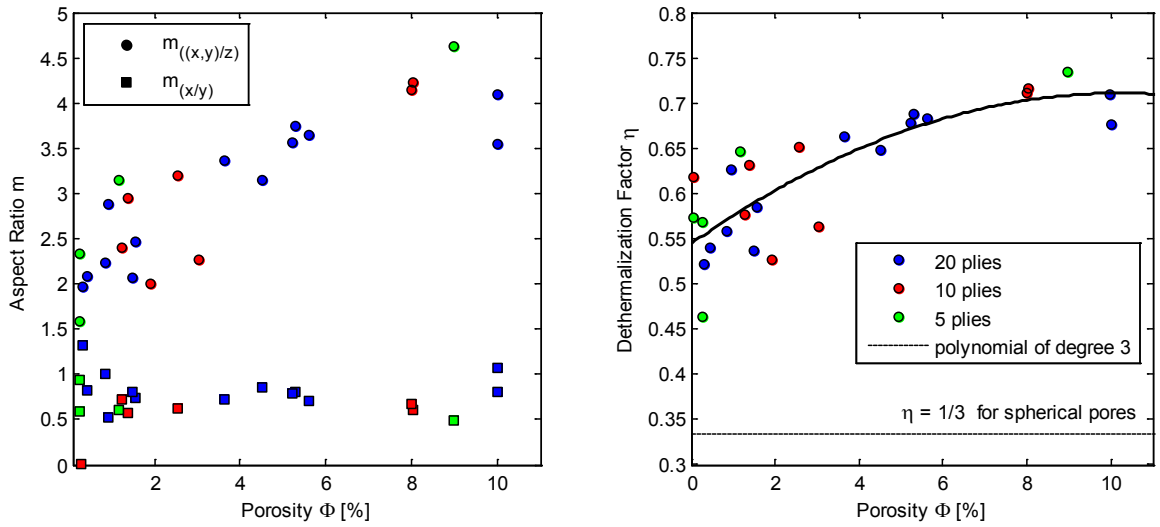

Fig. 8. *A plot of averaged in-plane and out-of-plane aspect ratios (left) and the calculated "dethermalization" factors based on Eq. 2 (right) of 20, 10 and 5 plies porosity samples versus porosity.*

5. Model-based porosity evaluation

In figure 9, the effective thermal diffusivity values obtained from experimental study of porous CFRP in transmission and reflection mode are compared with the predicted effective diffusivity values derived from Eq. 4 for fixed ($m = 1$) and porosity dependent ($m = f(\Phi)$) aspect ratios. For the prediction of the effective thermal diffusivity values the thermophysical properties given in table 2 were used.

Table 2. *Thermophysical properties of the CFRP constituents used for the effective medium approximation.*

Property		*Unit*	***Matrix***	***Pore***
Thermal conductivity	k	$W / (m\,K)$	0.7	0.026
Density	ρ	kg / m^3	1570	1.2
Heat capacity	c	$J / (kg\,K)$	1200	1000
Thermal diffusivity	α	m^2 / s	$3.72 \cdot 10^{-7}$	$2.17 \cdot 10^{-5}$

As seen from figure 9, the model-based thermal diffusivity values calculated with porosity dependent pore shapes $m = f(\Phi)$ predict the measured values up to 18 % fairly well especially for the 20 ply specimens measured in transmission mode. For all specimens with different number of plies (20, 10 and 5) the thermal diffusivity decreases roughly linearly with increasing porosity. For a 1 % porosity level there is approximately a 1.8 % decrease in the effective thermal diffusivity.

The relation between experimentally observed thermal diffusivity in transmission and reflection mode and predicted thermal diffusivity derived from the MG - Approximation shown in figure 10 demonstrates a good prediction capability despite of different number of plies. Especially with the 20 plies data in transmission mode the predicted values lie closer to the observed values, since there is a homogeneous pore distribution. In reflection mode, the deviation of the predicted values is slightly higher than in transmission mode.

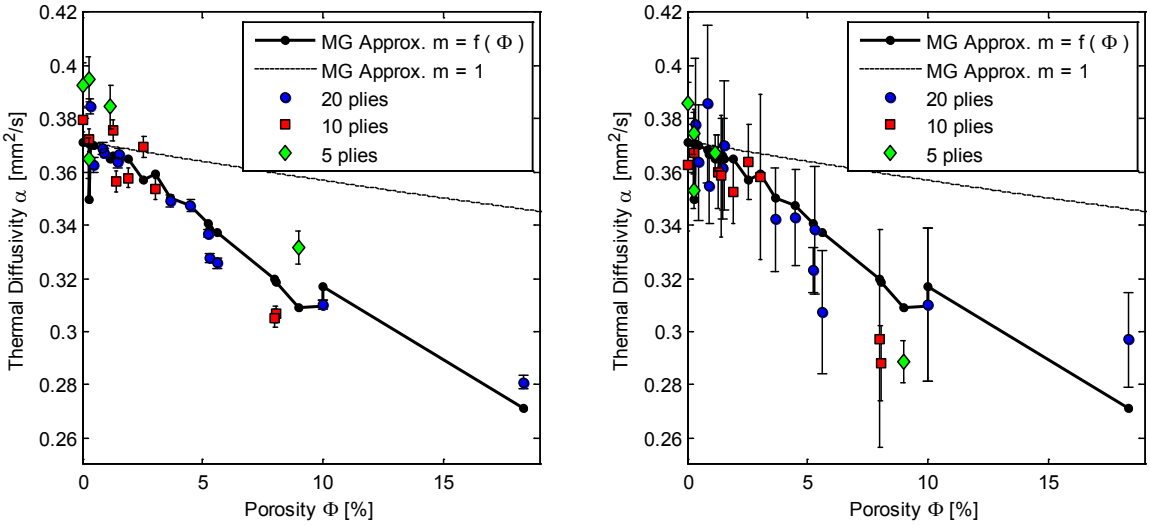

Fig. 9. *A plot of the calculated thermal diffusivities in transmission (left) and reflection mode (right) of 20, 10 and 5 plies porosity samples versus porosity obtained by 3D-XCT. The experimental data is compared to the Maxwell-Garnett Approximation.*

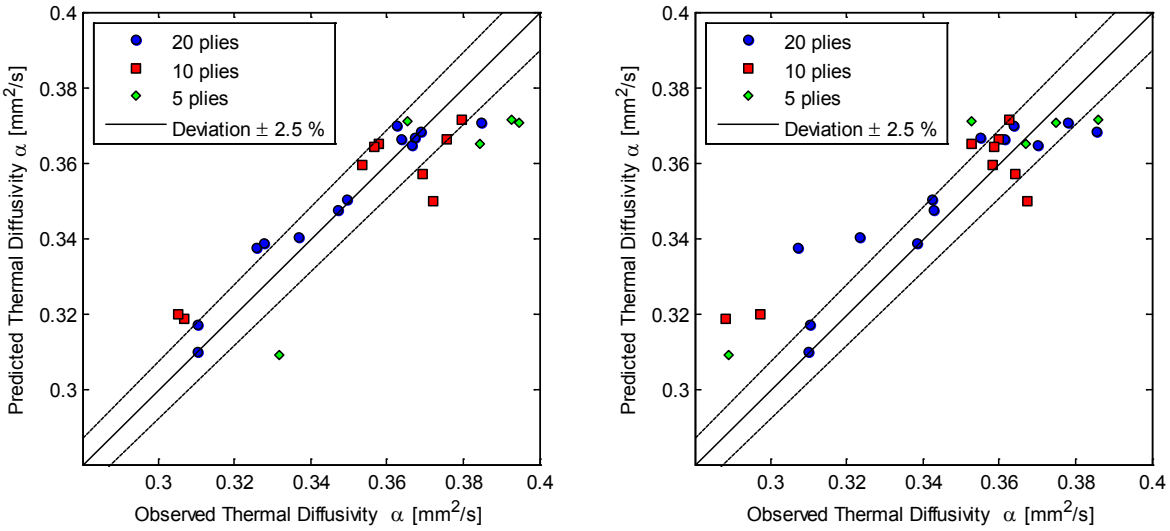

Fig. 10. *A plot of the observed thermal diffusivity in transmission (left) and reflection mode (right) of 20, 10 and 5 plies porosity samples and the predicted values by Maxwell-Garnett Approximation.*

Figure 11 shows how pulsed thermography in transmission and reflection mode can be used as a quantitative non-destructive evaluation tool for determining porosity in CFRP. By substituting the MG Approximation (Eq. 1) and the volumetric heat capacity average (Eq. 3) in Eq. 4 for the effective thermal diffusivity and rearranging this equation an explicit description of the porosity can be derived:

$$\Phi(\alpha) = \frac{1}{2a(M-P)\eta(k_m - k_p)} \times \Big(k_m \big(a(P - P\eta + M(2\eta - 1)) + k_m - \eta k_m \big) + \big(a(P - 2M)\eta + (\eta - 1)k_m \big) k_p - \Big((\eta - 1)^2 k_m^2 (k_m - k_p)^2 + \big(a(M + P(\eta - 1)) k_m - aP\eta k_p \big)^2 + 2ak_m (k_m - k_p) \Big((1-\eta)(P + P\eta - M)k_m + \eta(P + P\eta - 2M)k_p \Big) \Big)^{1/2} \Big) \tag{7}$$

where $M = (\rho\ c)_m$ is the volumetric heat capacity of the matrix and $L = (\rho\ c)_p$ of the pore. The following graph compares the 3D-XCT measured values of Φ with the values predicted by Equation 7. This shows that the predicted values and the measured values match one another quite well. For porosity levels higher than 0.5 % the transmission modes correlation coefficient $R^2 = 0.85$ is better than the reflection modes correlation coefficient $R^2 = 0.72$.

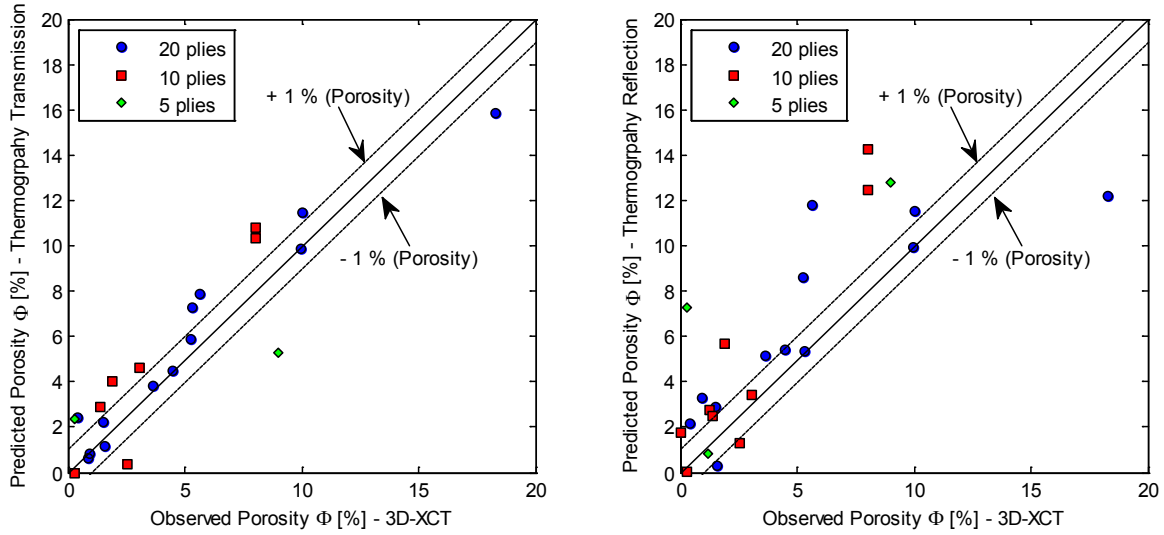

Fig. 11. *A plot of the predicted porosity levels based on pulsed thermography and Eq. 7 in transmission (left) and reflection mode (right) of 20, 10 and 5 plies porosity samples versus the exact porosity obtained by 3D-XCT measurements.*

6. Conclusion

Characterization of porosity in CFRP can be accomplished by thermal diffusivity measurements in both transmission and reflection mode. For a 1 % increase of the porosity level there is approximately a 1.8 % decrease in the effective thermal diffusivity. It has been demonstrated that it is possible to model this change in diffusivity with an effective medium approximation which is based on microstructure data derived from 3D-XCT measurements. The uncertainty of porosity characterization decreases with increasing sample thickness. In thicker samples more pores are present at the same porosity level, so that the heterogeneous material and the pore distribution can be treated as statistically homogeneous. This statistical homogeneity is a prerequisite for the application of the effective medium theory.

7. Acknowledgement

This work was financially supported by the TAKE OFF program of the Bundesministerium für Verkehr, Innovation und Technologie (BMVIT). Furthermore, we wish to thank our cooperation partner FACC AG and SECAR GmbH. XCT evaluations were supported by the Comet-project ZPT financed by FFG and the Government of Upper Austria.

REFERENCES

[1] Birt E. A. and Smith R. A., “A review of NDE methods for porosity measurement in fibre-reinforced polymer composites”, Insight, vol. 46(11), pp. 681-686, 2004.

[2] Daniel I. M., Wooh S. C. and Komsky I., “Quantitative porosity characterization of composite materials by means of ultrasonic attenuation measurements“, Journal of Nondestructive Evaluation, vol. 11(1), pp. 1-8, 1992.

[3] Connolly M. P., “The measurement of porosity in composite materials using infrared thermography”, Journal of Reinforced Plastics and Composites, vol. 11(12), pp. 1367-1375, 1992.

[4] Grinzato E. G., Marinetti S. and Bison P. G., “NDE of porosity in CFRP by multiple thermographic techniques", Proc. SPIE 4710, Thermosense XXIV, pp. 588-598, 2002.
[5] Zalameda J. N. and Winfree W. P., "Thermal diffusivity measurements on composite porosity samples", Review of Progress in Quantitative Nondestructive Evaluation, vol. 9, pp. 1541-1548, 1990.
[6] Ringermacher H. I., Howard D.R. and Gilmore RS., “Discriminating porosity in composites using thermal depth imaging”, AIP conference proceedings, vol. 615(1); 2002. p. 528–535.
[7] Ringermacher H. I. and Cassenti B. N., “Dethermalization Theory: Thermal/Dielectric analogy for heat flow through porosity in composites”, Journal of Nondestructive Evaluation, 2013, DOI 10.1007/s10921-013-0196-6.
[8] Mayr G., Plank B., Sekelja J. and Hendorfer G., „Active thermography as a quantitative method for non-destructive evaluation of porous carbon fiber reinforced polymers“, NDT&E International, vol. 44, pp. 537-543, 2011.
[9] Mayr G., Gruber J. and Hendorfer G., “Analytical and numerical computations of heat transfer in pulsed thermography applied to porous CFRP”, AIP conference proceedings vol. 1430, pp. 1025-1032, 2012.
[10] Maxwell J. C., “Treatise on Electricity and Magnetism”, Clarendon Press, Oxford, 1873.
[11] Kaviany M., “Principles of Heat Transfer in Porous Media”, Mechanical Engineering Series, 2nd ed., Springer, New York, 1995.
[12] Torquato S., “Random Heterogeneous Materials – Microstructure and Macroscopic Properties”, Chapman & Hall, London, 2002.
[13] Osborn J.A., “Demagnetizing factors of the general ellipsoid”, Physical Review, vol. 67(11-12), pp. 351-357, 1945.
[14] Kerrisk J. F., “Thermal Diffusivity of Heterogeneous Materials”, Journal of Applied Physics, vol. 42(1), pp. 267-271, 1971.
[15] Parker W. J., Jenkins, R. J., Butler, C. P. and Abbot, G. L., “Flash method of determining thermal diffusivity, heat capacity and thermal conductivity”, Journal of Applied Physics, vol. 32, pp. 1679-1684, 1961.
[16] Thermitus M.-A. and Laurent M., “New logarithmic technique in the flash method”. International Journal of Heat and Mass Transfer, vol. 40(17), pp. 4183-4190, 1997.
[17] Hendorfer G., Mayr G., Zauner G., Haslhofer M. and Pree R. "Quantitative determination of porosity by active thermography", AIP conference proceedings 894, pp. 702-708, Portland (Washington), 2006.
[18] Shepard S.M., Lhota J.R., Rubadeux B.A., Wang D., Ahmed T., “Reconstruction and enhancement of active thermographic image sequences”, Optical Engineering, vol. 42(5), pp. 1337-1342, 2003.
[19] Balageas D. L., "Thickness or diffusivity measurements from front-face flash experiments using the TSR (thermographic signal reconstruction) approach", Proceedings of 10th Quantitative InfraRed Thermography conference, paper QIRT2010-011 Québec (Canada), 2010.
[20] Kastner J., Plank B., Salaberger D. and Sekelja, J. "Defect and porosity determination of fibre reinforced polymers by X-ray computed tomography", Proceedings of the International Symposium on NDT in Aerospace, vol. 2, WE.1A.2, Hamburg (Germany), 2010.
[21] Winfree W. P. and Zalameda J. N. "Single sided thermal diffusivity imaging with a shuttered thermographic inspection system", AIP conference proceedings 615, pp. 544-551, Brunswick (Maine), 2002.
[22] Cilberto A., Cavaccini G., Salvetti O., Chimenti M., Azzarelli L., Bison P.G., Marinetti S., Freda A. and Grinzato E., “Porosity detection in composite aeronautical structures”, Infrared Physics & Technology, vol. 43, pp. 139-143, 2002.